FH | JOANNEUM
Luftfahrt / Aviation

Bachelor's Thesis

Large Eddy Simulation of Heat Transfer on Wing surfaces in 3D

Submitted by:	Stefan Lengauer
Registration number:	1210587029
Academic Assessor:	Dr.rer.nat. Wolfgang Hassler
Date of Submission:	16 March 2015

Declaration of Academic Honesty

I hereby affirm in lieu of an oath that the present bachelor's thesis entitled

"Large Eddy Simulation of Heat Transfer on Wing Surfaces in 3D"

has been written by myself without the use of any other resources than those indicated, quoted and referenced.

Graz, 16 March 2015

Stefan LENGAUER,

Preface

This thesis was written as part of my bachelor's degree program at FH Joanneum, University of Science in Graz, Austria.

One of the challenges in the conduction of this project was the location of the necessary hardware, which was at the department's facility. This required a physical attendance at the university for the majority of the work. Also the literature research proved difficult, since there is not yet that much material covering this specific topic.

With regard to this obstacles I am satisfied with the outcome of this project and I hope to provide the reader with a broad overview on the basics of Large Eddy Simulation as well as its advantages and disadvantages.

Thus I want to thank everyone who supported me writing this thesis.

Contents

Abstract

Large Eddy Simulation, a subdomain of Computational Fluid Dynamics, is recently experiencing an increased attention, due to increasing capabilities of the necessary hardware, in detail CPU and memory. In most sectors it is not yet industrial standard, because of its height demand in terms of resources, but it will most likely become an important tool for the investigation of complex flow problems in near future.

Therefore this bachleor's project compromises the execution of a high-resolution simulation of the heat transfer on a wing surface in three dimensions. The given geometry for this task is a NACA 0012 airfoil and the used software tools are Ansys ICEM and Ansys CFX.

Subsequent the achieved results are compared to results obtained from a similar RANS simulation, which is nowadays standard for industrial application. Based on this evaluation the applicability of LES is scrutinized and discussed.

Kurzfassung

Large Eddy Simulation, ein Teilbereich der numerischen Strömungsmechanik, erfährt in letzter Zeit erhöhte Beachtung dank der steigendenden Leistungsfähigkeit der erforderlichen Hardware, insbesondere CPU und Speicher. In den meisten Bereichen ist sie aufgrund ihres hohen Ressourcenaufwandes noch nicht Industriestandart, aber in naher Zukunft wird sie ein wichtiges Instrument zur Untersuchung von komplexen Strömungsproblemen werden.

Aus diesem Grund beinhalted dieses Bachelorprojekt die Durchführung einer hochauflösenden Simulation eines Wärmeübergangs an einem dreidimensionalen Flügelprofil. Die, für diese Aufgabe gegebene Geometrie, ist ein NACA 0012 Flügelprofil und die verwendeten Softwarepakete beinhalten Ansys ICEM und Ansys CFX.

Anschließend werden die erzielten Resultate mit den Resultaten einer vergleichbaren RANS Simulation verglichen, welche momentan Standart für industrielle Anwendungen sind. Diese Auswertung dient als Grundlage für die darauffolgende Untersuchung und Diskussion der Anwendbarkeit der Large Eddy Simulation.

List of Figures

List of Symbols

c_p	Specific heat coefficient, J/kg K
k	Turbulent kinetic energy, m^2/s^2
ε	Turbulent energy dissipation rate, m^2/s^3
ϑ	Velocity scale, m/s
l	Length scale, m
ρ	Density, kg/m^3
μ_{SGS}	Dynamic sub grid scale viscosity, kg/m s
μ_t	Turbulent viscosity, kg/m s
ν	Kinematic viscosity, m^2/s
ν_t	Turbulent kinematic viscosity, m^2/s
λ	Heat conductivity, W/K m
Nu	Nußelt number, dimensionless
Re	Reynolds number, dimensionless
Pr	Prandtl number, dimensionless
Fr	Froude number, dimensionless
C_D	Drag coefficient, dimensionless
$F_{horizontal}$	Force in horizontal direction, kg m/s^2
σ	Stefan-Boltzmann constant, W/ m^2 K^4
τ_{ii}	Normal stresses, N/m^2
δ_{ij}	Kronecker symbol, dimensionless
Δ	Cutoff width, m
Q	Heat, J
h_c, α	Heat transfer coefficient, W/m^2 K
T_0	External boundary temperature, K
T_w	Walltemperature, K
q_w	Heat flux at wall boundary, W
q_{cond}	Heat flux caused by convection, W
q_{rad}	Heat flux caused by radiation, W
v	Characteristic velocity, m/s

η	Dynamic viscosity, kg/m s
y^+	Dimensionless wall distance, dimensionless
u_τ	Frictional velocity, m/s
τ_w	Wall shear stress, N/m^2
U	Mean flow velocity, m/s
Δy_1	First cell height, m
A_{eff}	Area facing in flow direction, m^2
Δt	Temperature difference, K
R_{LE}	Airfoil nose radius, m
t	Maximum profile height, m

List of Tables

List of Abbreviations

CAD	Computer Aided Design
CDS	Central Difference Scheme
CFD	Computational Fluid Dynamics
DES	Detached Eddy Simulation
DNS	Direct Numerical Simulation
GS	Grid Scale
GUI	Graphical User Interface
HPC	High Performance Computing
HPCC	High Performance Computing Cluster
LES	Large Eddy Simulation
RANS	Reynolds-averaged Navier Stokes
SGS	Sub Grid Scale
SST	Shear-Stress Transport
VLES	Very Large Eddy Simulation

Chapter 1

Introduction

The academic discipline of CFD (Computational Fluid Dynamics) emerged in the 1970s as alternative to the experimental and the theoretical approach for the prediction of flows. It relies on the physical modeling of a flow as mathematical problem which is then solved numerical. Nevertheless compared to other computer aided engineering domains it lagged behind for a long time due to the tremendous complexity of the underlying models for the description of fluid flows, which should be at the same time economical and physical sufficient correct. Although it comes with huge hardware costs, especially for the LES (Large Eddy Simulation), it is usually still more economical than an experimental facility and features various advantages like the capability of the investigation of very large systems, or systems under hazardous conditions [1].

The LES is a subdomain of the CFD and features dedicated filters which reject the smaller eddies and let the larger ones pass. This is done prior to the computation, where the smaller eddies are represented by turbulence models. The LES is usually more effort to implement and wrong choices of the models often lead to strong deviations of the results.

The analysis and prediction of turbulent flows is a critical factor for the comprehension of natural and technical flow processes. This basis is necessary for the improvement of objects surrounded by a flow like aircraft.

This chapter starts off with the basics of turbulent flows before it covers the technical principles of LES and heat transfer.

1.1 Basics of turbulent flows

Turbulences appear in a great range of shapes and sizes. Independent of their complexity, all flows become unstable above a certain Reynolds number. While they are usually laminar at low Reynolds numbers they become more and more turbulent, when it increases [2]. This specific value at which the flow turns over from laminar to chaotic is called critical Reynolds number [1].

Turbulences have always three-dimensional, spacial character, even if the velocities and pressures vary just in one or two dimensions. The typical signs of turbulence are the so-called turbulent eddies which are basically rotational flow structures as they can be seen in figure 1.1. The eddies come with a wide range of various length- and time scales and due to their rotational flow fields, particles which are initially separated by long distances can be brought together quickly, which leads to a high efficiency in terms of heat, mass and momentum exchange [1].

Although turbulent flows are highly chaotic and almost impossible to predict over longer periods of time, the characteristic lengths of the large eddies are proportional to the considered flow problem. An important term which has to be considered in this context is the energy cascade, which is widely known as Kolmogorov's energy cascade, named after the Russian scientist, who described these circumstances as first. In a typical turbulent flow kinetic energy is handed down from the large scale eddies, which are by far the most energetic ones, to the smaller ones. Figure 1.2 shows the spectral energy of eddies dependent on their wavenumber. The wavenumber is given by $\kappa = 2\pi/\lambda$, with λ as the wavelength of the eddies. Obviously the smaller eddies hold by far the least energy. The larger scales get their energy from the mean flow and break up in the smaller scales. The Reynolds number of the smaller scales equals one, which means that the inertia and the viscous effects are of equal strength. All the work they perform is against the viscous stresses and accordingly all the energy they hold dissipates into internal thermal energy [1, 2].

1.2 CFD attempts to deal with turbulence

In CFD there are different ways in order to deal with turbulent flows. All natural flows are more or less turbulent, but in the computation the turbulences are usually resolved

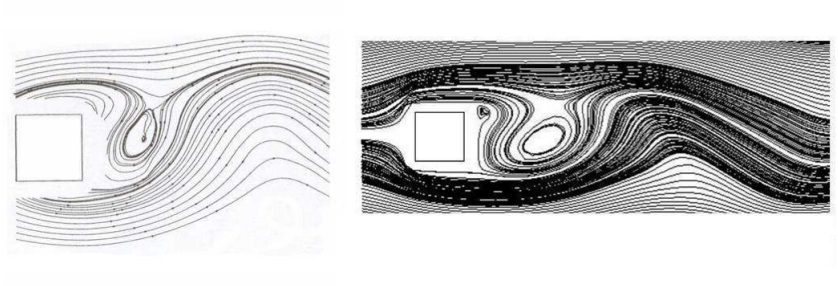

Figure 1.1: [5, p.13] Experimental and numerical streamlines

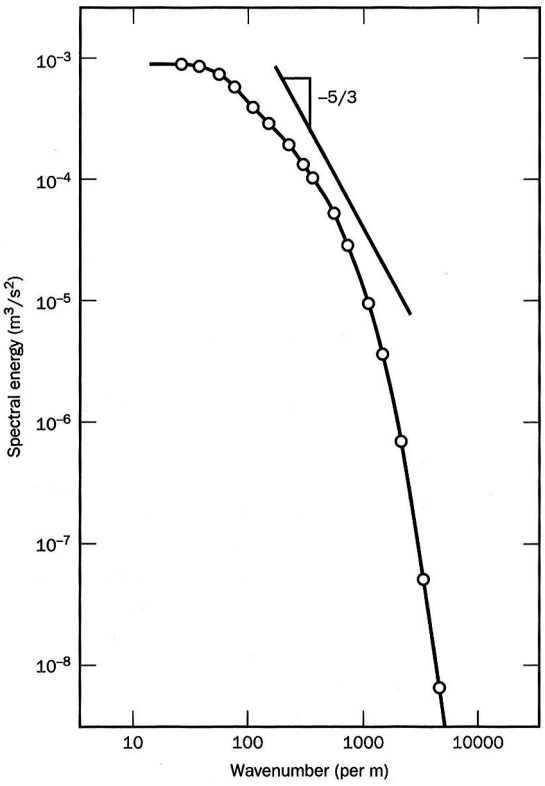

Figure 1.2: [1, p.43] Energy spectrum of turbulence of different scales

only to a certain degree or omitted altogether. Methods for calculation of flows can be organized according to their turbulence resolving capability.

The so called RANS (Reynolds Averaged Navier-Stokes) equations are the most common and wide-spread approach in order to deal with any flow prediction. This method yields time averaged properties of the flow like mean velocities, mean pressures, mean stresses, etc. For many technical flow investigations this is satisfying and therefore this simulation type has been the method of choice for CFD calculations for the past decades. Other advantages are the modest demand on resources and the fact that two-dimensional calculations are sufficient. The RANS equations for incompressible flows lead to six additional stresses, known as the Reynolds stresses. This

stresses are unknown and for computing turbulent flows they need to be predicted by dedicated turbulence models like the $k - \varepsilon$ model.

With DNS (Direct Numerical Simulation) all scales of turbulence are simulated numerical. Therefore a three-dimensional grid is needed, which is at least as fine as the smallest scale eddy. Additionally the time step needs to be small enough to resolve even the fastest fluctuation. This leads to tremendous requirements in terms of computing power and mesh quality and therefore it is usually performed only for academic researches on rather small and simple geometries.

The LES represents a sort of compromise between RANS equations and DNS. It has also high demands on storage and CPU performance for unsteady and transient flows need to be computed. But still, it is less demanding than DNS and due to the fast improvement of hardware this method becomes more and more applicable, even for more complex flow problems. As the title suggest, this project concentrates mostly on this kind of simulation and therefore it will be discussed in more detail in the following.

There exist also a lot of sub-forms and mixtures of various approaches, like DES (Detached Eddy Simulation), VLES (Very Large Eddy Simulation), etc. However, to mention them here would go beyond the scope of this report.

For the project the RANS and the LES simulation have been applied. This chapter is dedicated to introduce the reader to some crucial basics of LES. It will cover the terms fine structure model and turbulence model. Due to the numerous different models and approaches, each subchapter will deal only with the methods used for this particular project [1, 2].

1.3 Basic idea of Large Eddy Simulation

Although there have been huge efforts for developing turbulence models since the early days of CFD, a model suitable for a wide range of practical applications and offering convincing results still does not exist. This is due to the very different properties of the various scales of eddies. The smaller eddies are almost isotropic and show universal behavior while the larger ones interact with and extract energy from the main flow. Their behavior is heavily dependent on the used geometry and the boundary conditions. The core principle of LES is that the larger eddies are computed with a time dependent simulation, while the smaller scales are still represented by models. How-

ever, since the smaller scales are breakdown products of the larger one and represent just a small amount of the overall energy, they are easier to model. With Reynolds-averaged equations on the other hand *all* scales need to be represented by a single turbulence model, which proves to be inaccurate, especially for the larger eddies.

The classification of *small* and *large* eddies is conducted with dedicated filter functions, which take a *cutoff* width as input parameter. When applied the filter function destroys all the information related to the eddies which are beyond this scale, while the rest remains untouched and gets computed. To describe this association the terms GS (grid scale) and SGS (sub-grid scale) are used. When the smaller scales are left out, also their effects on the flow are omitted. This effects are known as SGS stresses and have to be described by means of so-called SGS models, which are basically turbulence models.

The finer the applied filter is, the more eddies are modeled numerically and therefore the FS model can be simpler while yielding a similar accurate solution. If the filter becomes, theoretically, indefinitely small, the LES fades into a DES. The other margin case would be a very rough filter, which allows only the most energized eddies. This kind of simulation is known as VLES (Very Large Eddy Simulation).

These circumstances offer two possible options in order to improve the simulation. There can be improved either the FS model or the used grid. In most cases an improvement of the FS model is the option of choice, since a refinement of the grid leads to a much higher demand in terms of resources and comes with no warranty to provide a more accurate solution. However, one should bear in mind that, a LES is also highly dependent on the preceding inlet circumstances as well as the wall functions [1, 3].

1.4 Turbulence models

A majority of the scientific research concerning LES is dedicated to the development of the so called fine structure- or turbulence models. They are used to represent the impact of SGS eddies symbolically, by dissipating as much energy as it would be the case with a DNS model of the same problem. Most of the fine structure models used today are deterministic. Accordingly they are dependent of the velocity field and yield exactly one solution [1].

1.4.1 $k-\varepsilon$ turbulence model

The $k-\varepsilon$ models are the most frequently used and best proved turbulence models for RANS equations. The reason for their popularity is their convincing performance in confined flow, what is usually the case with industrial application. For these simulations the $k-\varepsilon$ model offers a good compromise between accuracy and robustness. In contrast to its excellent performance for many industrially relevant flows, it shows some major weaknesses when it comes to unconfined or rotating flows.

The standard $k-\varepsilon$ model presumes an isotropic turbulent viscosity and adds two extra transport equations, one for the k and one for the ε, which need to be solved alongside the RANS flow equations. The first transported variable k stands for the turbulent kinetic energy, while the ε term is responsible for the dissipation and features the dimensions m^2/s^3. With k and ε the velocity scale ϑ and the length scale l are defined as $\vartheta = k^{1/2}$ and $l = k^{3/2}/\varepsilon$. Through this identity the eddy viscosity can be obtained by

$$\mu_t = C\rho\vartheta l = \rho C_\mu \frac{k^2}{\varepsilon} \tag{1.1}$$

where C_μ is a dimensionless constant. The additional equations for k and ε are then:

$$\frac{\partial(\rho k)}{\partial t} + div(\rho k U) = div\left[\frac{\mu_t}{\sigma_k} grad k\right] + 2\mu_t S_{ij} S_{ij} - \rho\varepsilon \tag{1.2}$$

$$\frac{\partial(\varepsilon k)}{\partial t} + div(\rho\varepsilon U) = div\left[\frac{\mu_t}{\sigma_\varepsilon} grad\varepsilon\right] + C_{1\varepsilon}\frac{\varepsilon}{k} 2\mu_t S_{ij} S_{ij} - C_{2\varepsilon}\rho\frac{\varepsilon^2}{k} \tag{1.3}$$

The left side of the equation deals with the rate of change of k or ε plus the transport of by convection, while the right side features the transport by diffusion plus the rate of production minus the rate of destruction of the values k and ε. C_μ, σ_k, σ_ε, $C_{1\varepsilon}$ and $C_{2\varepsilon}$ are constants with given values for the standard $k-\varepsilon$ model that are applicable for a wide range of turbulent flows [1].

1.4.2 Smagorinsky-Lilly SGS model

The Smagorinsky-Lilly SGS model bases on the assumption that the turbulent stresses are proportional to the mean rate of strain. This approach requires the changes in the flow direction to be slow in order to balance the production and dissipation of turbulence. Furthermore the turbulence structures should be isotropic [1].

> "Thus, in Smagorinsky's SGS model the local SGS stresses R_{ij} are taken to be proportional to the local rate of strain of the resolved flow $\bar{S_{ij}} = \frac{1}{2}(\partial\bar{u_i}/\partial x_j + \partial\bar{u_j}/\partial x_i)$:" [1, p.102]

This leads to the equation

$$R_{ij} = -2\mu_{SGS}\bar{S_{ij}} + \frac{1}{3}R_{ij}\delta ij = -\mu_{SGS}\left(\frac{\partial\bar{u_i}}{\partial x_j} + \frac{\partial\bar{u_j}}{\partial x_i}\right) + \frac{1}{3}R_{ii}\delta_{ij}. \tag{1.4}$$

The additional term on the right hand side of the equation is responsible that the formula yields the correct results for the normal stresses τ_{xx}, τ_{yy} and τ_{zz}. Due to the definition of the Kronecker symbol δ_{ij}, this term becomes zero for any other stresses. The constant which determines the relation between local stresses and local rate of strain is the dynamic SGS viscosity μ_{SGS}. The Smagorinsky-Lilly model bases on Prandtl's mixing length model, which comes with the assumption that the kinematic turbulent viscosity ν_t can be expressed through the velocity scale ϑ and the turbulent length scale l by

$$\nu_t = C\vartheta l. \tag{1.5}$$

Here C is a dimensionless constant of proportionality. The dynamic viscosity μ_{SGS} can then simply be obtained by $\mu_{SGS} = \nu_{SGS}\rho$. For the length scale the cutoff width Δ, used for the filter, is the logic choice.

Hence the dynamic SGS viscosity can be taken as

$$\mu_{SGS} = \rho(C_{SGS}\Delta)^2|\bar{S}| = \rho(C_{SGS}\Delta)^2 sqrt2\bar{S_{ij}}\bar{S_{ij}} \tag{1.6}$$

Various studies proved that values between 0.1 and 0.24 for the constant C_{SGS} are appropriate, but occasionally this parameter needs adjustment in order to provide reasonable results [1].

1.5 Heat transfer

Heat is a special form of energy and is stored in the chaotic movement of atoms and molecules. In a non-adiabatic system it is the amount of energy which resigns over the border if a temperature gradient is prevailing. The transition of the heat over the system borders is therefore called heat flux and runs always in the direction of the

lower temperature [4].

Basically there are three different ways how heat can be transferred from one system to another. In practical application they usually appear combined but for computation they can be dealt with individually. Each of them will be discussed in the following.

1.5.1 Mecanisms of heat transfer

With *conduction*, heat gets transferred between particles in immediate vicinity. It occurs with adjacent molecules of solids or steady fluids. If no counteracting processes are present the temperature difference becomes sooner or later zero. The heat conduction through a solid wall can be described by means of *Fourier's law*:

$$Q = \frac{\lambda}{\delta} A \Delta t \tau \tag{1.7}$$

The heat conductivity λ is a material property and dependent from the temperature. δ is the thickness of the wall and τ the timespan.

Between moving fluids proceeds the so-called *convection*. This form of heat transfer is the dominant one in liquids and gases. It occurs in two different forms. As *free convection*, if the heat transfer itself causes the flow, which would for example be the case if air flows by a heating device. Or as *forced convection* if the movement is caused by device like a pump or a fan. This would be the case when cooling an engine.

The last form of heat transfer is by *radiation*. Radiation is the transmission of energy by means of waves. It can proceed through different materials, although no material is required for it is also capable of spreading through space. Physically, the internal energy of the radiating system is converted into multiple tiny energies, which are then emitted. The movement and location of the single photons cannot be determined, but the behavior of a mass of photons can be described by means of an electromagnetic wave. Usually the radiation is named after its way of creation, like γ-, or x-radiation. The specific radiance M of a body is given by

$$M = \varepsilon \sigma T^4 \tag{1.8}$$

, where ε is the emission coefficient and can be taken from dedicated tables. σ is a physical constant called Stefan-Boltzmann constant with a fixed value of 5.87e-8 [4].

1.5.2 Wall heat flux in Ansys CFX

The most important property, which will be investigated within this project is the wall heat flux. In Ansys CFX this variable represents the total heat flux into the domain, which consists of convective and radiate participations.

The heat flux at a wall boundary is specified by a heat transfer coefficient h_c, which is obtained from the equation

$$q_w = h_c(T_0 - T_\omega) = q_{rad} + q_{cond} \tag{1.9}$$

where T_0 is the external boundary temperature and T_ω is the temperature at the wall, which is provided explicitly in this project. Figure 1.3 visualises this circumstances [8].

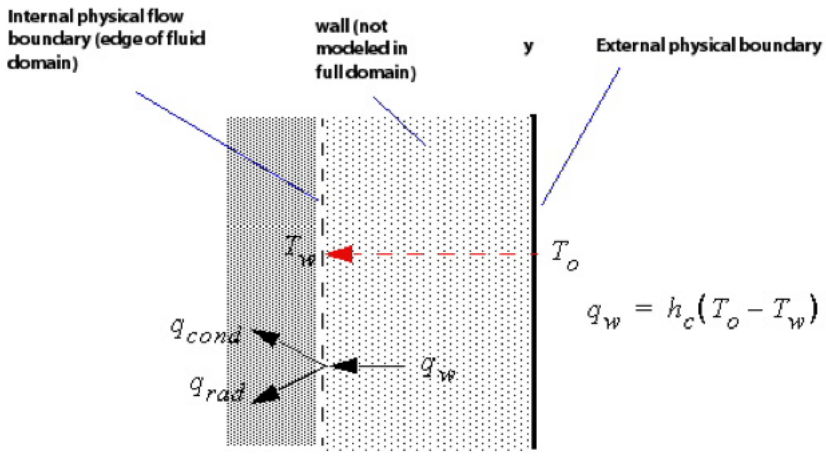

Figure 1.3: [8] Heat transfer model in Ansys CFX

1.6 Similitude of heat transfer

It is impossible to determine the heat transfer for every technical problem experimentally. Fortunately, it is possible to transfer existing results to physically similar objects from which the heat transfer coefficient can then be obtained.

The originator of this similitude theorem is Wilhelm Nußelt. The Nußelt number, which is a form of the differential equation of the heat transfer, but with dimensionless parameters, is named after him. It is the dimensionless form of the heat transfer

coefficient and given by

$$Nu = \frac{\alpha l}{\lambda} \tag{1.10}$$

Once the Nußelt number of a specific problem is known the heat transfer coefficient α can be easily calculated. The Nußelt number itself is dependent from other dimensionless numbers which describe flow- and heat transfer processes. The most important ones are the Reynolds number and the Prandtl number. The Reynolds number is capable of predicting similar flow patterns in different fluid flow situations and is defined as

$$Re = \frac{vl}{\nu} \tag{1.11}$$

where v is the characteristic velocity of the fluid, l a characteristic length of the problem (for example the inner radius of a pipe, which is flowed through by a fluid), and ν the kinematic viscosity of the fluid.

The Prandtl number is named after the German physicist Ludwig Prandtl and defined as

$$Pr = \frac{\eta c_p}{\lambda} \tag{1.12}$$

with η for the dynamic viscosity of the fluid, c_p as the specific heat and λ as the thermal conductivity. As a heavily on temperature dependent material property, it can be often found in tables of heat transfer properties. For air and many other gases a Prandtl number of 0.7 to 0.8 is common under normal circumstances. Unlike the Reynolds number, the Prandl number contains no length scale variable, but is dependent only on the fluid and the fluid state. For forced convection the Nußelt number is a function of the Reynolds- and the Prandtl number.

$$Nu = Nu(Re, Pr) \tag{1.13}$$

For many technical applications and problems the functional relation of these parameters is known. The value of the Nußelt number at the stagnation line of a cylinder with laminar flow for example is given by

$$Nu = 1.14 Pr^{0.4} Re^{0.5} \tag{1.14}$$

The Nußelt number and thus the heat transfer coefficient α increases with the Reynolds

number. This leads to an improved heat transfer at higher velocities. Table 1.1 shows, reachable, as well as for practical application common values, for the heat transfer coefficient [4].

Table 1.1: [4, p.374] Typical values for the heat transfer coefficient

	Acquireable values	Common values
Gases		
-Free convection	5 ... 25	8 ... 15
-Forced convection	12 ... 120	20 ... 60
Fluids		
-Free convection	70 ... 700	200 ... 400
-Forced convection	600 ... 12,000	2,000 ... 4,000

Chapter 2

Methods

The first section of this chapter deals with the resources used for the project, while the subsequent ones focus completely on setting up the CFD software tools and executing the actual simulation. The subchapters are divided according to the different parts of software or properties they are dealing with.

2.1 Technology used

CFD is an area with huge demands in computing power. Therefore industrial CFD calculations belong to the domain of supercomputers or HPCCs (high performance computing clusters). Everything needed for the conduction of this project in terms of hard- and software was provided in the FH Joanneum facility.

2.1.1 Hardware

The department of Aviation at the University of Applied Sciences in Graz is equipped with a HPC (high performance computing) laboratory, compromising sixteen high performance computers, capable of providing the huge amount of CPU power needed for CFD calculations.

Table 2.1 shows the properties of one of these devices.

Table 2.1: Specification of computing hardware

Central Processing Unit (CPU)	Intel® Xeon(R) CPU X5690
Architecture	x86_64
Core speed	1596 MHz
Cores	12
Random Access Memory (RAM)	23.6 GB

2.1.2 Software

The computers in the HPC laboratory feature the operating system Debian 7.8 (wheezy). Each has the software packages ANSYS ICEM CFD 14.0 and ANSYS CFX 15.0 installed, which were used for performing the simulation. Additionally, minor calculation, as well as the analysis and visualization of the results was done with MATLAB®.

ANSYS ICEM CFD 14.0 is an effective software tool for generating, improving and repairing CAD (Computer Aided Design) meshes. Its primary function however is the generation and enhancement of meshes, which are necessary for the flow simulation. Therefore it allows the import from various different CAD software and is able to export the mesh for several different CFD solvers such as ANSYS CFX.

ANSYS CFX 15.0 is the software tool used for conducting the simulation. It is a high-performance CFD program for many different fluid flow problems and comes with a highly potent and intuitive GUI. There are three different subprograms for individual simulation tasks. *ANSYS CFX 14.0 Pre* is responsible for setting up initial conditions, solver settings and the like, while *ANSYS CFX-Solver Manager 14.0* deals with the actual solving of the equations for the individual meshes and time steps. The third one, *ANSYS CFX CFD-Post 14.0*, is used for the post-processing and analysis of finished calculations and is capable of three-dimensional visualization of the results, as well as performing various calculations and drawing charts.

The following subchapters are divided according the software tools, used for the particular steps.

2.2 Mesh generation with Ansys ICEM 14.0

The meshed NACA 0012 airfoil was provided as two-dimensional C-grid domain by Dr. Hassler as it can be seen in figure 2.1. It is meshed with hexahedral elements and features a total of 219,000 elements. The domain features physical measurements

of 7m by 5m by 0.01m and the wing profile inside the domain comes with a chord length of 1m. Due to the nature of the profile with a maximum thickness of 12%, the thickness is 0.12m in total values. On the left side is located the inlet, on the right the outlet and the upper and lower borders are defined as walls, as it can be seen in figure 2.1. Figure 2.2 features a close-up on the enormous grid refinement at the airfoil surface.

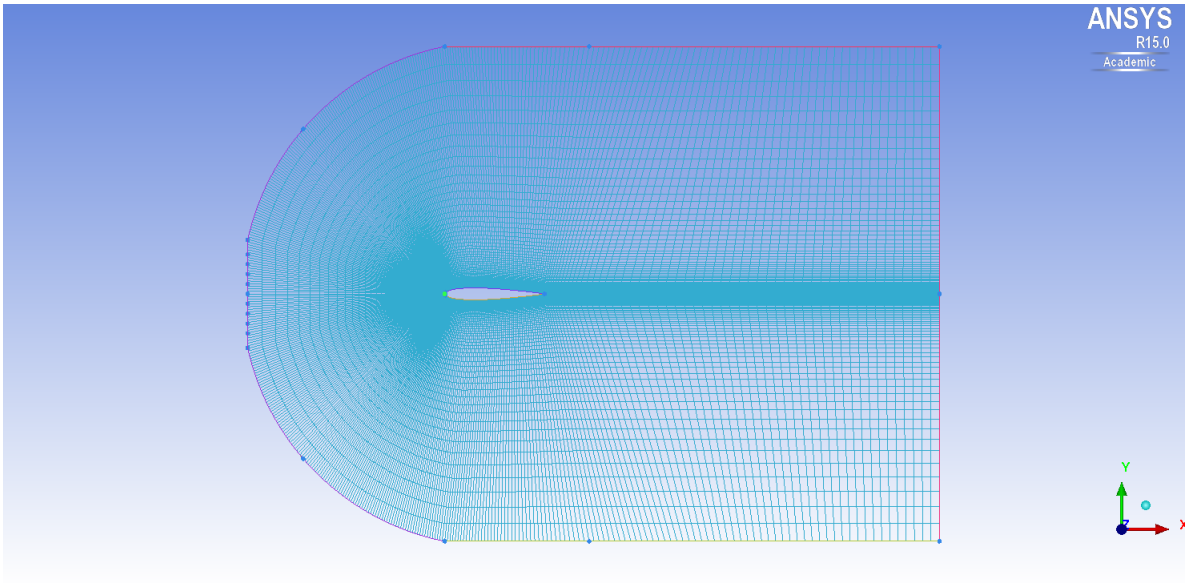

Figure 2.1: Provided domain with mesh refinement in vicinity of the wing surface

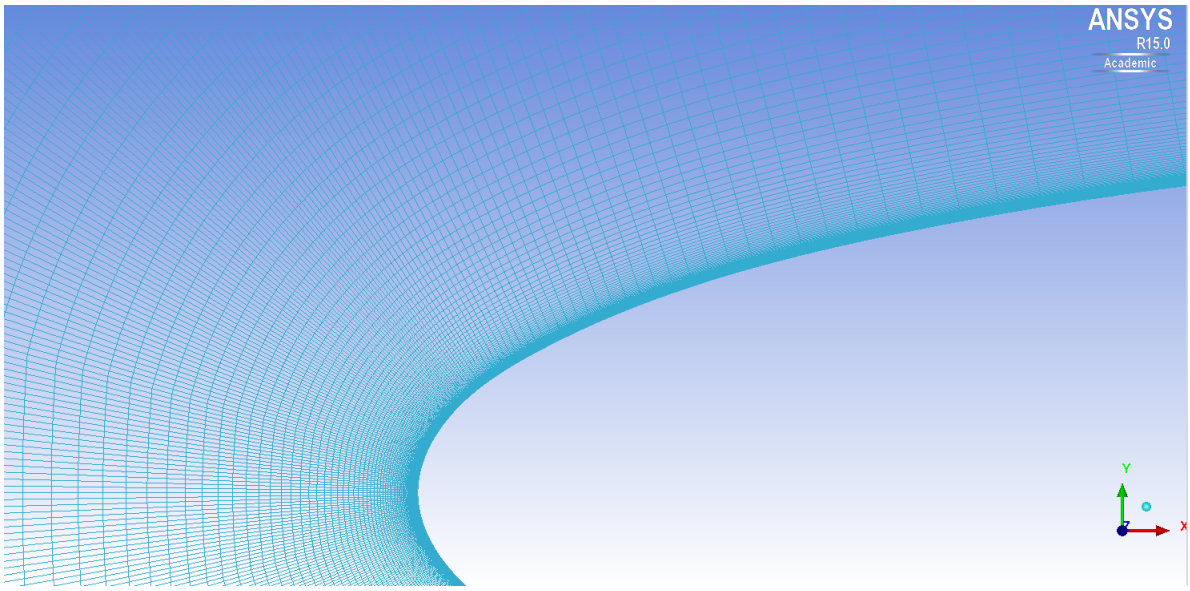

Figure 2.2: Close-up to the mesh at the airfoil surface

Due to the three-dimensional characteristics of the large eddies this two-dimensional mesh was not sufficient, but had to be extended in the third dimension in order to be capable of providing convincing results. This was achieved by simply extending the

given mesh in the third direction by thirty elements, resulting in a physical thickness of 0.30m in z-direction. This leads to a total of 2,263,000 elements and 2,172,810 nodes. In figure 2.3 the final mesh is visible in an isometric view with the airfoil in the center. The properties of the final mesh, as it was exported from Ansys ICEM 15.0 are listed in table 2.2.

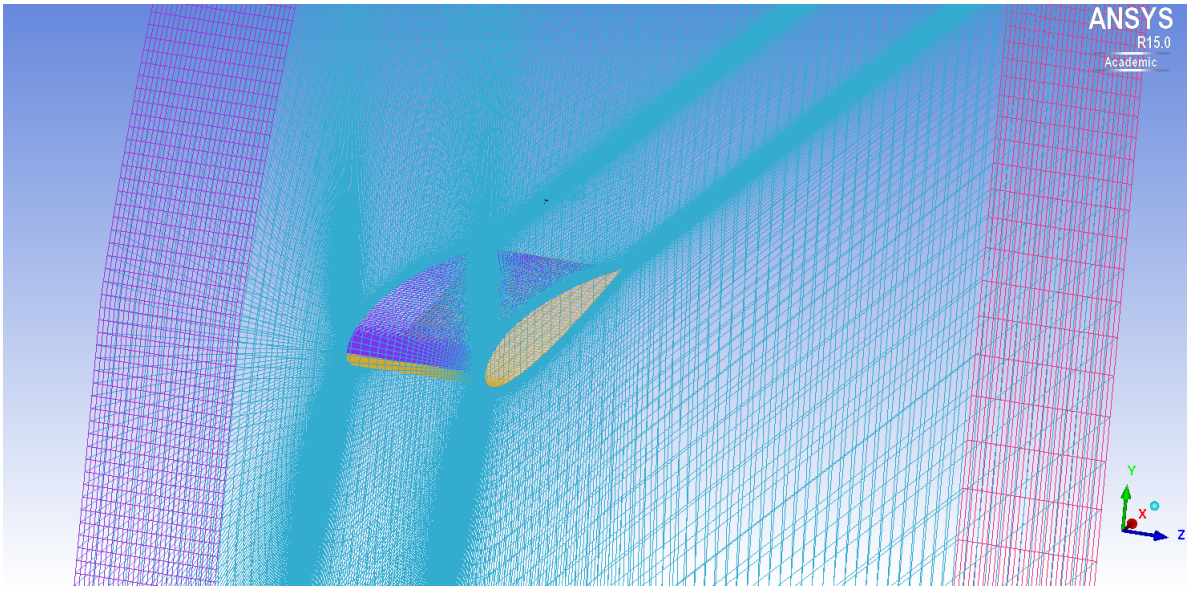

Figure 2.3: Close-up of the meshed geometry in isotropic view

Table 2.2: Properties of the mesh

Domain length	7m
Domain height	5m
Domain width	0.3m
Profile chord length	1m
Maximum profile thickness	0.12m

2.2.1 y⁺ value

The y^+ value is the dimensionless wall distance and an important factor for evaluating the physical accuracy of the flow in vicinity of a wall. It is connected with the frictional velocity u_τ and the kinematic viscosity ν by

$$y^+ = \frac{\rho u_\tau y}{\mu} \tag{2.1}$$

with y for the orthogonal offset from the wall. u_τ is then given by

$$u_\tau = \sqrt{\frac{\tau_w}{\rho}} \tag{2.2}$$

The wall shear stress τ_w can be obtained by the following formula

$$\tau_w = \frac{1}{2} C_f \rho U^2 \tag{2.3}$$

with C_f as the skin friction coefficient which must be taken from empirical results, ρ as the density and U as the mean velocity of the main flow. A good estimation for internal flows is $C_f = 0.079 Re^{-0.25}$.

For the Large Eddy Simulation it is crucial to score a y^+ value at around 1.0 or below. In order to evaluate the height of the first cell, necessary to achieve a certain y^+ value equation 2.1 can be transformed to

$$\Delta y_1 = \frac{y^+ \mu}{\rho u_\tau} \tag{2.4}$$

with the first cell height Δy_1.

Although the y^+ value is dependent from time and location for simple geometries and flows, such as the one used for this rough estimate, this correlation is highly accurate [1, 2, 7].

For the calculation of the Δy_1 value a short MATLAB® script has been applied. It yielded a result of 8.02e-6 for the height of the cell in immediate vicinity of the wing surface. An investigation of the given geometry in Ansys ICEM 15.0 (figure 2.4) showed that the height of this cell features a cell height of 9.55e-7, which is already beneath the desired value and therefore a refinement of the two-dimensional mesh was not necessary.

2.3 Simulation setup in Ansys CFX-Pre 15.0

There have been two simulations set up in Ansys CFX-Pre, linked together with *Simulation Control*. The first one was a stationary RANS simulation with the task to provide a fully developed flow field as initial condition for the subsequent LES. In Ansys CFX-Pre they were entitled according to their simulation type “Stationary” and “Transient”.

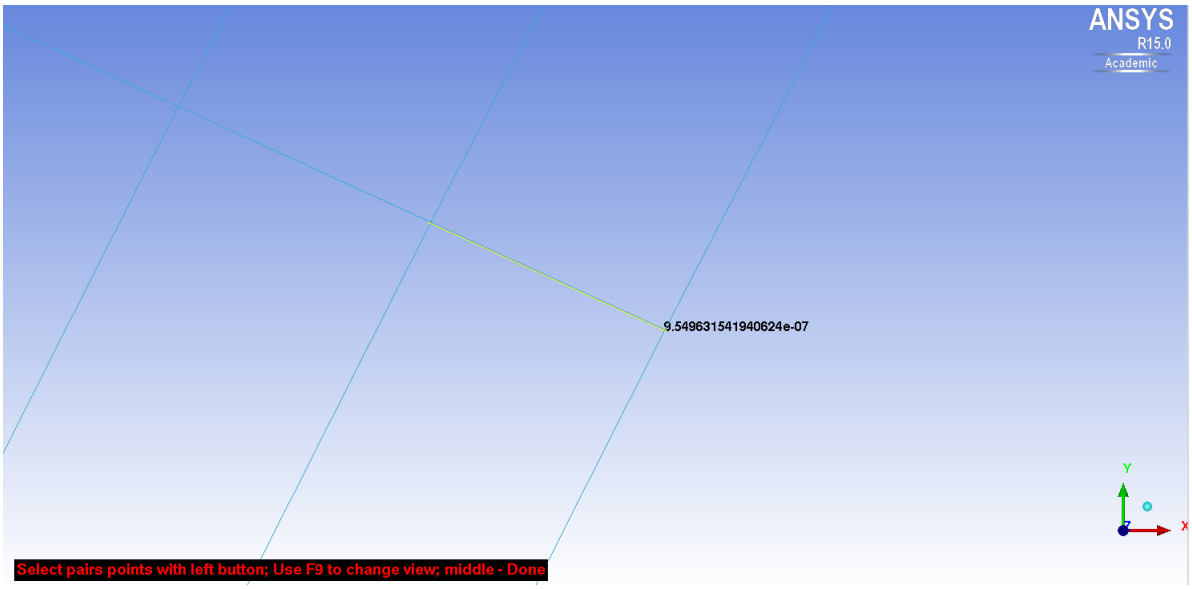

Figure 2.4: Measurement of the height of the cell next to the wing surface

Each simulation has the properties described in the following chapters for themselves. However, since they are mostly the same for either simulation, there will be no strict distinction between the two of them, but it will be referred to explicitly, if there have been differences in the adjustments.

2.3.1 Domain

The CFD software requires a specific area where the equations for each method can be evaluated. Usually the object of interest is located inside the domain and at the borders of a domain are applied so-called boundary conditions, responsible of defining the borders of the area of investigation. In Ansys CFX one or more fluid models can be defined for a domain. These are used to describe and adjust the fluid dominating in this area. For this project only one fluid model was necessary, featuring air at twenty-five degrees. The turbulence model of the fluid however was different for stationary- and transient simulation. While the stationary one was based on the $k - \varepsilon$ model, the transient applied the LES Smagorinsky model.

2.3.2 Analysis type

For the transient analysis a number of time steps and duration of the time steps themselves had to be considered. For the amount of time steps an initial quantity of 20,000 was chosen. For adjusting the necessary time step value the so-called CFL (Courant-

Friedrichs-Lewy) number was investigated, which proves to be a good measurement for accuracy. In order to provide reliable and stable results an average CFL number in the range of 0.5 to 1.0 is demanded. There are also stable results possible with higher CFL number, but the turbulences may be damped and the result distorted.

After starting the solving with various different timstep values it settled on a value of 1e-5 seconds, which lead to an equivalent Courant number of 0.87.

2.3.3 Boundary conditions

In total there have been seven boundary conditions defined. The first one is for the inlet conditions and provides a constant inlet velocity at the western front of the domain. Instead of an outlet, an opening was specified on the eastern border. This is the option of choice for turbulent flows, allowing backflows of the fluid to reenter the domain, instead of just leaving. The northern and southern walls were defined as free-slip walls and the wing surface as no-slip wall, leading to a velocity of zero on surface of the wing. Two symmetry conditions at the front- and the backside completed the closure, simulating a theoretical infinite expansion in z-direction.

2.3.4 Initial conditions

As initial inlet velocity, 66.8m/s was specified. Furthermore the relative pressure was set to zero, meaning that the initial pressure in the domain equals the pressure prevailing at the outlet. In Simulation Control it was declared that the LES simulation uses also the developed flow field of the preceding RANS simulation as initial condition.

2.3.5 Solver control settings

For the Advection Scheme for the LES was chosen *Specific Blend Factor*. This scheme allows using a mixture of the High Order Advection Scheme and the CDS (Central Difference Scheme). The relation between these two techniques is controlled via the Blend Factor [10]. For the start a Blend Factor of 0.5 was chosen, meaning that the schemes were used in equal shares. In advance of the solving this factor was altered according to table 2.3, in order to favor more and more the CDS, which would have been the intended choice for the transient simulation.

Another setting needed for transient simulations is the number of coefficient loops. This is the maximum number of times the equations are iterated for a single time step.

> "The implicit coupled solver used in CFX requires the equations to be converged within each timestep to guarantee conservation. The number of coefficient loops required to achieve this is a function of the timestep size. With CFL numbers of order 0.5-1, convergence within each timestep should be achieved quickly. It is advisable to test the sensitivity of the solution to the number of coefficient loops, to avoid using more coefficient loops (and hence longer run times) than necessary." [9]

As an initial setting the number of maximum coefficient loops has been set to 10. However, if the size of the time step requires more than tree to five coefficient loops the result can be considered as inaccurate. As convergence criteria a root mean square of below 1e-6 of the residual target has been demanded. This can be considered as the minimum required accuracy for a LES in order to achieve scientific relevant results.

Table 2.3: Adjustment of the blend factor with respect to the time step interval

Time step interval	Blend factor
1 ... 10,000	0.5
10,001 ... 15,000	0.3
15,001 ... 18,555	0.1

2.3.6 Output control

Due to numerous time steps and the resulting large amount of data, only the results of every tenth time step have been permanently saved to the disk. Moreover the output of the *Transient Results* have been limited to the properties Pressure, Wall Heat Flux and Force in x-direction for further decreasing the necessary storage. For easy recovery after a shutdown or the like, a full backup has been conducted automatically every hundredth time step.

2.3.7 Simulation control

The sequence of the simulations and their relationship has been specified by means of the *Simulation Control*. The stationary simulation was executed first with given initial

conditions. The transient simulation followed subsequent and was able to benefit from the fully developed flow field of the preceding simulation.

2.4 Solving with Ansys CFX-Solver-Manager 15.0

The solver setup has been specified as full run with double precision checked in order to receive more exact results. The chosen technique was Intel MPI Distributed, which allows the usage of multiple machines on the local network. In total six computers of type described in table 2.1 have been applied for executing the solving.

Due to the provided settings the solver started with the stationary simulation, which finished normally. Thereafter the transient one was conducted. It was aborted after 18,555 time steps, because a review of the latest results showed that the simulation has already reached a kind of steady state and thus no more time steps were needed. In total it took 1.307e6 seconds (15 days, 3 hours, 3 minutes, 58 seconds) to calculate all 18,555 time steps and writing 1,855 transient result files and 185 backup files.

Chapter 3

Results

With a time step duration of 1e-5 seconds all time steps combined make up a physical simulation duration of 0.19s. Although this seems to be a rather short timespan, it proves to be sufficient, because with a velocity of 66.8m/s the flow passes the wing surface with a length of 1m five times during this simulation time.

The content of this chapter deals with the investigation of the last 200 time steps.

3.1 Checking accuracy requirements

The post-processing was conducted with Ansys CFX-Post 15.0. The first thing was checking whether the y^+ value on the wing surface was within the correct scope. This was done by plotting the value on the wing surface as it can be see in figure 3.1. Obviously it is nowhere beyond one and hence this requirement is fulfilled.

Additionally the drag coefficient of the wing was mirrored over the last time steps. When it does not change any more, it can be assumed that the simulation has reached a kind of steady state. The value for the drag coefficient was calculated in Ansys CFX-Post by the equation [5]

$$C_D = \frac{F_{horizontal}}{\frac{1}{2}\rho U^2 A_{eff}} \tag{3.1}$$

where A_{eff} is the projection of the wing geometry in flow direction and $F_{horizontal}$ the force operating in x-direction. The values for the drag coefficient for the last 200 steps are listed in table 3.1. It can be seen that they stay the same, apart from some minor deviations.

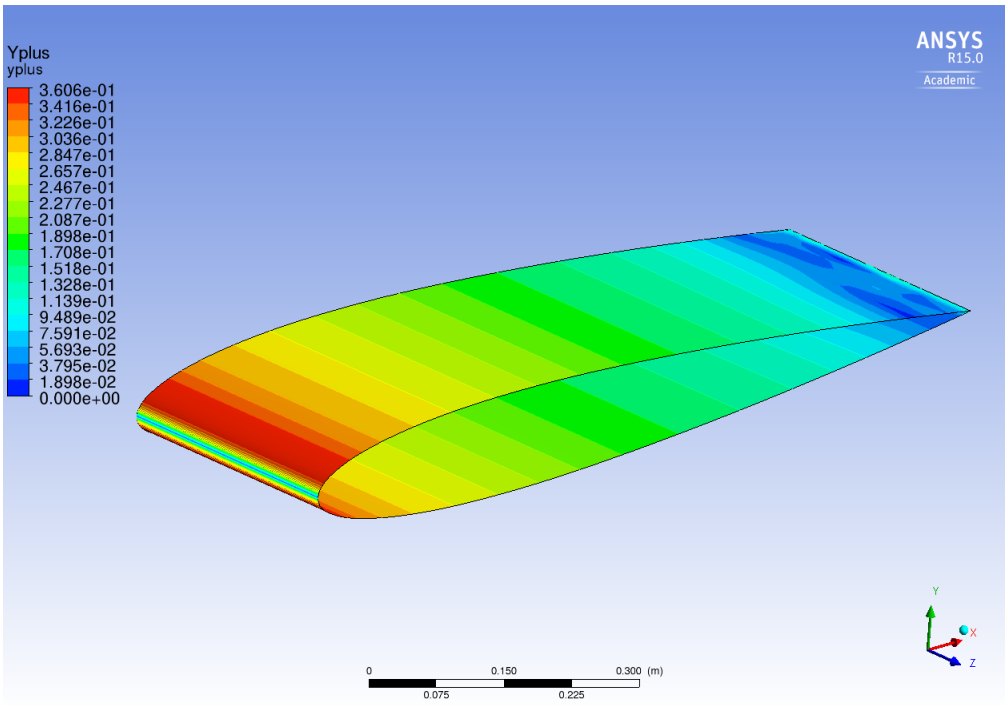

Figure 3.1: The y^+ value on the airfoil surface

3.2 Exporting data from Ansys CFX-Post

For investigating the heat transfer a polyline was inserted exactly at the middle of the airfoil. It was obtained by intersecting the wing surface with a xy-plane, which was positioned at 0.15m in z-direction. Subsequent the properties x-coordinate and Wall Heat Flux on this polyline were exported as csv file. This file served as input for MATLAB® and was used for the visualization of the results.

For comparison and evaluation purpose the same flow problem was simulated by Dr. Hassler by means of a RANS simulation. The result file of this simulation was treated the same way, so that there could be exported a csv file with the stationary data as well.

3.3 Processing in MATLAB®

As next step the csv files were imported into MATLAB®, where the data was extracted and used for plotting the wall heat flux over the length of the profile. For comparison reasons both results, the stationary as well as the transient one, were displayed in the same plot, which can be observed in figure 3.2.

This data for the heat transfer was the basis for the calculation of diverse dimen-

Table 3.1: Variation of the drag coefficient over the last 200 time steps

Time step	Drag coefficient
18,450	0.104639763906978
18,460	0.104639857472925
18,470	0.104639857472925
18,480	0.104640124290383
18,490	0.104640333687198
18,500	0.104640527598881
18,510	0.104640735058614
18,520	0.104640635962194
18,530	0.104640528407586
18,540	0.104640719551398
18,550	0.104640922019082

sionless numbers, which were of major importance for the evaluation of the simulation. In detail, the Nußelt and the Froude number were used for comparison. For a cylinder the Froude number is more or less equal to one. This was utilized for the evaluation, because the nose of the airfoil can be compared to a cylinder. The Nußelt and Froude number have been computed with three different approaches. For the first, the Nußelt number for a cylinder, equal to the airfoil nose diameter, was generated by means of the Prandtl and the Reynolds number with the relation given in equation 1.14. This was done for comparison reason with a typical specific heat transfer coefficient of 1,005 Joules per kilogram Kelvin applied. For the other two approaches the Nußelt number was computed from the values extracted from the simulation. Particularly the values of the wall heat flux at the stagnation point, where x is equal to zero, were of special interest. The stationary simulation yielded a value of 253.69 Watt per square meter at this point and the transient one a value of 257.05 Watt per square meter. These were used for computing the heat transfer coefficient α, which can be obtained through the correlation

$$\alpha = \frac{q}{\Delta t} \tag{3.2}$$

with Δt as the difference of the temperatures of wall and fluid [4]. With respect to the initial settings it was one degree. The airfoil nose diameter served as specific length scale, given by the radius $R_{LE} = 1.1019t^2$ times two, with t as the maximum profile height. The Nußelt number was then calculated by means of equation 1.10. In table 3.2 the differences and similarities of the single approaches can be observed.

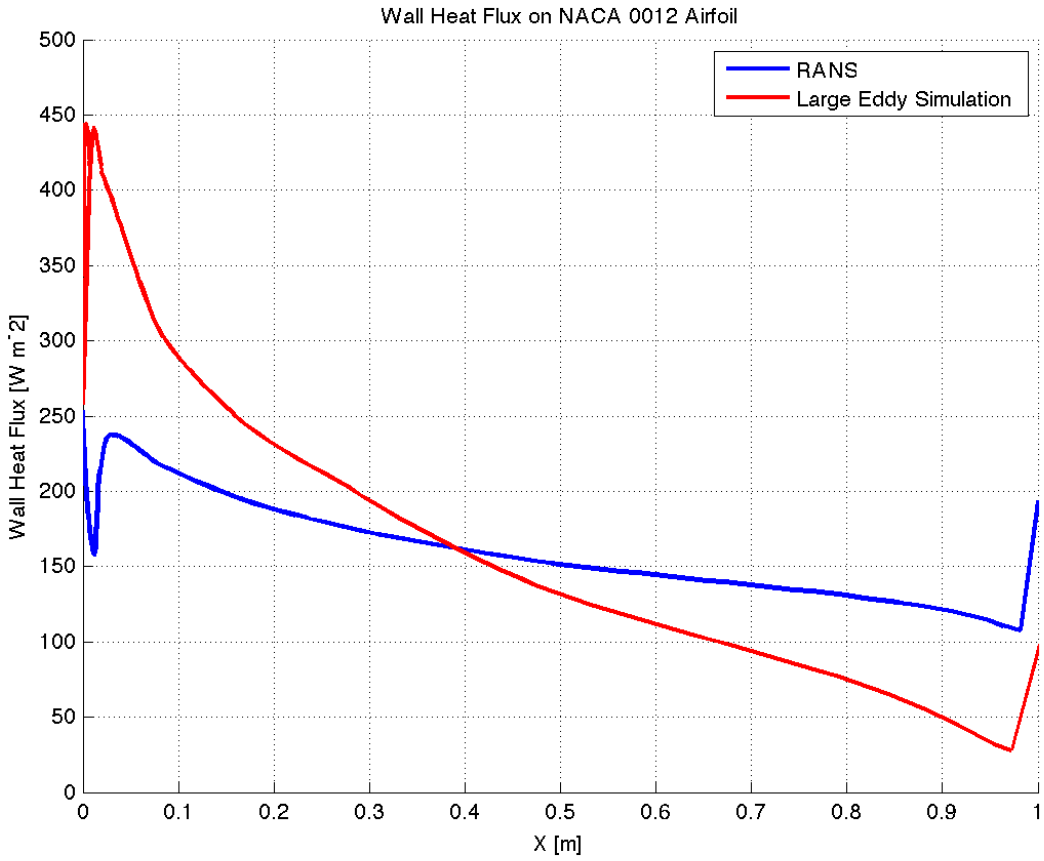

Figure 3.2: Distribution of the wall heat flux on the wing surface along the x-axis

Table 3.2: Dimensionless coefficients resulting from the simulation

	Values for a cylinder	RANS results	LES results
Reynolds number		134,000	
Prandtl number	0.7141	-	-
Nußelt number	364.72	308.94	313.03
Froude number	0.9963	0.8439	0.8551
α, W/m^2 K	257.05	253.69	299.50

Chapter 4

Discussion

As mentioned in the abstract the aim of this project is the conduction of a heat transfer by means of a Large Eddy Simulation, afterwards comparing the obtained results with the results of a RANS simulation of the same flow problem and analyzing deviations and similarities, as well as evaluating the applicability of the LES for technical flow investigation.

4.1 Investigation of the wall heat flux

As basis for the inspection and evaluation served the wall heat flux on the wing surface. The examination relied on the results obtained from the simulations, which are plotted in Figure 3.2 and the calculation results, belonging to them, in table 3.2. Although in this plot it seems like there is just one graph per simulation type, there are actually two for each - one for the upper side and one for the bottom side of the wing. However, due to the symmetry of the geometry and the flow conditions their heat transfer along the profile is almost the same, appart from minor numerical inaccuracies.

The heat transfer resulting from the RANS equations features a heavy flunctuation at the front end of the airfoil. This is physically illogically and results most likely from the application of the SST (Shear-Stress Transport) turbulence model for this simulation. The LES results seem more convincing in this respect and it can be oberved that they feature a much higher wall heat flux at the front section of the wing and a lower one at the rear section, while it is equal to the stationary simulation at about forty percent wing depth. This agrees with the exectations, because in a turbulent flow the heat transfer is much better than in a laminar flow for the turbulent vortices movement favors the

energy exchange [1].

4.1.1 Interpretation of the dimensionless numbers

This subchapter is dedicated to analysing of the dimensionless number refered to in table 3.2. The Reynolds number is of course the same for all solutions since it is independent from heat transfer. The parameter of interest is the Foude number, which is almost equal to one for a cylinder. For the transient solution the Froude number shows a deviation of about fourteen percent from this value. What causes this inaccuracy may be the subject of further investigations, but an interesting fact here is, that it is still closer to the desired result than the stationary simulation.

4.1.2 Comparison Large Eddy Simulation and RANS equation

As already mentioned the Large Eddy Simulation requires massive resources and a very sophisticated mesh compared to the RANS equations. However there are significant reasons, why LES becomes more and more attractive than RANS. One major drawback of the RANS equations is, that they are not sufficiently reliable in terms of prediction of heat transfers, as it is the case with this simulation, where the RANS equations come up with a physically rather questionable behavior of the heat transfer distribution.

On the other hand one should be aware of that a slightly inappropriate modelling of the LES can easily lead to completely wrong results. Accordingly LES requires a deeper knowlege of the subject, but in return it is capable of dealing with plenty of different flow conditions, without relying on a priori assumptions [1, 3].

Chapter 5

Conclusion

Unfortunately there were nowhere experimental results of a heat transfer on a NACA airfoil to be found and therefore the LES method could only be evaluated by comparing with other CFD results. Accordingly one interesting task for future investigations would be the comparison of the results from this project to experimentally achieved results.

Furthermore it has to be stated that the documentation and reference material for the Large Eddy Simulation is rather meager and it seems that the Ansys Software tool are more dedicated to stationary simulations. Due to the long calculation durations it appears rather cumbersome and errors in the simulation setup can cost a vast amounts of time. Therefore it became obvious that LES requires more experience and knowledge in CFD in order to produce reliable results

Nevertheless there are various reasons to prefer the LES, as stated in chapter 4.1.2, and thus it is most likely to become more frequently applied for technical flow investigation in the future.

Bibliography

[1] Versteeg, H.K., and Malalasekera, W., *An Introduction to COMPUTATIONAL FLUID DYNAMICS: The Finite Volume Method, 2nd ed.*, Pearson Education Limited, Harlow, England, 2007.

[2] Hassler, W., "Numerische Berechnungsverfahren (CFD-Teil)", 2012.

[3] Fröhlich, J., *Large Eddy Simulation turbulenter Strömungen, 1st ed.*, Teubner Verlag, Wiesbaden, 2006.

[4] Cerbe, G., and Wilhelms, G., *Technische Thermodynamik: Theoretische Grundlagen und praktische Anwendungen, 15th ed.*, Carl Hanser Verlag, München, 2008.

[5] Ochoa, J.S., and Fueyo, N., "Large Eddy Simulation of the flow past a square cylinder," Zaragoza, Spain.

[6] Anderson, D., and Tsao, J., "Evaluation and Validation of the Messinger Freezing Fraction," Ohio Aerospace Institute, Brook Park, Ohio, 2003.

[7] LEAP CFD Team, "Tips & Tricks: Estimating the First Cell Height for correct Y+," [web site], URL: http://www.computationalfluiddynamics.com.au/tips-tricks-cfd-estimate-first-cell-height/ [cited 12 March 2015].

[8] SAS IP, Inc., "Heat Transfer," [web site], URL: http://www.arc.vt.edu/ansys_help/cfx_mod/i1301427.html [cited 12 March 2015].

[9] SAS IP, Inc., "The Large Eddy Simulation Model (LES)," [web site], URL: http://www.arc.vt.edu/ansys_help/cfx_
mod/i1303019.html [cited 15 March 2015].

[10] ANSYS, Inc., "ANSYS CFX-Solver Theory Guide,", Southpointe, 2009.

Appendix A

Appendix

```
%%%%%%%%%%%%%%%%%%%%%%%%%%%%%%%%%%%%%%%%%%%%%%%%%%%%%%%%%%%%%%%%%%%%%%%%%%%%%%%
%
% Title:            cell_height.m
% Version:          2.2
% Author:           Stefan Lengauer
% Date:             16th February 2015
% Description:      File for computing the necessary cell height for the
%                   cells attached to the wing surface.
%
%%%%%%%%%%%%%%%%%%%%%%%%%%%%%%%%%%%%%%%%%%%%%%%%%%%%%%%%%%%%%%%%%%%%%%%%%%%%%%%

clear all;
close all;

% Definition of variables
rho = 1.168;     % Density, [kg m^-3]
U = 66.8;        % Velocity, [m/s]
L = 1;           % Characteristic length scale, [m]
mu = 18.48e-6;   % Dynamic viscosity [Pa*s]
yplus = 1;       % y+, dimensionless

Re = rho * U * L / mu;
Cf = 0.079 * power( Re, -0.25 );

Tau_w = 1/2 * Cf * rho * power( U, 2 );

Utau = sqrt( Tau_w / rho );
Δy = yplus * mu /( rho * Utau );
```

```
%%%%%%%%%%%%%%%%%%%%%%%%%%%%%%%%%%%%%%%%%%%%%%%%%%%%%%%%%%%%%%%%%%%%%%%%%%%%%%%
%
% Title:              wall_heat_flux_plot.m
% Version:            1.0
% Author:             Stefan Lengauer
% Date:               15th February 2015
% Required Files:     wall_heat_flux_stationary.csv
%                     wall_heat_flux_transient.csv
% Description:        Script for creating and saving the data plots
%                     obtained from CFX-Post.
%
%%%%%%%%%%%%%%%%%%%%%%%%%%%%%%%%%%%%%%%%%%%%%%%%%%%%%%%%%%%%%%%%%%%%%%%%%%%%%%%

clear all;
close all;

%% Data Import
STAT = csvread( '../simulation_data/wall_heat_flux_stationary.csv' );
TRANS = csvread( '../simulation_data/wall_heat_flux_transient.csv' );

x_stat = STAT( :, 1 );
y_stat = STAT( :, 4 );

x_trans = TRANS( 3:350, 1 );
y_trans = TRANS( 3:350, 4 );


%% Plot
hold on;
grid;

plot( x_stat, y_stat, 'linewidth', 2, 'color', 'blue' )
plot( x_trans, y_trans, 'linewidth', 2, 'color', 'red' )

axis( [0, 1, 0, 500] );
title( 'Wall Heat Flux on NACA 0012 Airfoil' )
legend( 'RANS', 'Large Eddy Simulation' )
xlabel( 'X [m]' )
ylabel( 'Wall Heat Flux [W m^-2]' )

%% Save Plot
saveas( figure(1), '../images/Wall_Heat_Flux_Plot.png', 'png' )
```

```
%%%%%%%%%%%%%%%%%%%%%%%%%%%%%%%%%%%%%%%%%%%%%%%%%%%%%%%%%%%%%%%%%%%%%%%%%%%%%%%
%
% Title:            dimensionless_coefficients.m
% Version:          1.3
% Author:           Stefan Lengauer
% Date:             3rd March 2015
% Description:      Script for computation for the dimensionless
%                   coefficients, necessary for the evaluation of the
%                   results.
%
%%%%%%%%%%%%%%%%%%%%%%%%%%%%%%%%%%%%%%%%%%%%%%%%%%%%%%%%%%%%%%%%%%%%%%%%%%%%%%%

clear all;
close all;

% Simulation parameters

c = 1.0;                % Chord length, [m]
t = 12/100;             % Maximum profile height, [m]
w = 66.8;               % Fluid velocity, [m s^-1]

tw = 26 + 273.15;       % Temperature at the wing surface, [K]
tf = 25 + 273.15;       % Temperature of the fluid, [K]
A = 0.5967;             % Wing surface, [m^2]
whf_trans = 257.0520;   % Wall heat flux at stagnation point from transient
                        % simulation, [W m^-2]
whf_stat = 253.6925;    % Wall heat flux at stagnation point from
                        % stationary simulation, [W m^-2]

% Material properties for air at 25C

cp = 1007;              % Heat transfer coefficient, [J kg^-1 K^-1]
eta = 18.48e-6;         % Dynamic viscosity, [kg m^-1 s^-1]
lambda = 26.06e-3;      % Thermal conductivity, [W K^-1 m^-1]
ypsilon = 15.82e-6;     % Kinematic viscosity, [m^2 s^-1]



R_LE = 1.1019 * power( t, 2 );  % Radius Leading edge, [m]
l = R_LE * 2;                   % Characteristic length scale, [m]


% Reynolds number
Re = w * l / ypsilon;

%% Theoretical values according to the fluid properties

% Prandtl number
Pr_id = cp * eta / lambda;

% Nusselt number
Nu_id = 1.14 * power( Pr_id, 0.4 ) * power( Re, 0.5 );

% Froude number
Fr_id = Nu_id / power( Re, 0.5 );

% Heat transfer coefficient
alpha_id = Nu_id * lambda / l;
```

```
%% Values with the Heat Transfer coefficient obtained from the transient
% simulation

% Heat transfer coefficient
alpha_stat = whf_trans / ( tw - tf );

% Nusselt number
Nu_stat = alpha_stat * l / lambda;

% Froude number
Fr_trans = Nu_stat / power( Re, 0.5 );

%% Values with the Heat Transfer coefficient obtained from the stationary
% simulation

% Heat transfer coefficient
alpha_stat = whf_stat / ( tw - tf );

% Nusselt number
Nu_stat = alpha_stat * l / lambda;

% Froude number
Fr_stat = Nu_stat / power( Re, 0.5 );
```

```
%%%%%%%%%%%%%%%%%%%%%%%%%%%%%%%%%%%%%%%%%%%%%%%%%%%%%%%%%%%%%%%%%%%%%%%%%%%%
%
% Title:            drag_coefficient.m
% Version:          1.3
% Author:           Stefan Lengauer
% Date:             13th February 2015
% Required Files:   force_x_18450.csv
%                   force_x_18460.csv
%                   force_x_18470.csv
%                   force_x_18480.csv
%                   force_x_18490.csv
%                   force_x_18500.csv
%                   force_x_18510.csv
%                   force_x_18520.csv
%                   force_x_18530.csv
%                   force_x_18540.csv
%                   force_x_18550.csv
% Description:      Script for computing the drag coefficient of the
%                   airfoil for the last 100 timesteps.
%
%%%%%%%%%%%%%%%%%%%%%%%%%%%%%%%%%%%%%%%%%%%%%%%%%%%%%%%%%%%%%%%%%%%%%%%%%%%%


rho = 1.1839;           % density of air at 25 degrees, [kg m^-3]
u = 66.8;               % inlet speed, [m s^-1]
max_thickness = 0.12;   % max thickness of the profile, [m]
width = 0.3;            % profile width, [m]


% initialization of the coefficient vector
CD = zeros( 1, 11 );

for i = 450:10:550
    file = strcat( '../simulation_data/force_x_18', int2str( i ), ...
        '.csv' );
    A = csvread( file );
    force_x = A(:,4);

    % computation of the drag coefficient
    index = ( i - 450 )/10 + 1;
    CD(index) = sum( force_x ) / ...
        ( 1/2 * rho * power( u, 2 ) * width * max_thickness );
end
```